Analysis of spatiotemporal signals of complex systems

C. Uhl, R. Friedrich, and H. Haken
Institut für Theoretische Physik und Synergetik, Universität Stuttgart, Pfaffenwaldring 57/IV, 70550 Stuttgart, Germany
(Received 27 June 1994; revised manuscript received 27 December 1994)

We present a method of analyzing spatiotemporal signals emerging from nonequilibrium self-organizing systems that are close to instability. The algorithm aims at an identification of spatial modes and corresponding order-parameter equations. We discuss and demonstrate the method by examples of simulated codimension I and II instabilities, including a numerically integrated partial differential equation leading to "blinking states."

PACS number(s): 05.90.+m, 02.60.−x

I. INTRODUCTION

In various fields of science the analysis of spatiotemporal patterns emerging from complex systems is an important element of research. The aim is to obtain a microscopic description of the system in terms of spatial patterns and their dynamics. Fields of application can vary from hydrodynamics (e.g., [1]), chemical reactions, and meteorology (e.g., [2]) to biological systems, such as the analysis of EEG [3,4] and MEG data [5,6]. One hopes to draw conclusions from the experimentally obtained macroscopic patterns to the microscopic level and to obtain a deeper insight into the cooperation of various components of a nonequilibrium system [7].

Up to now there seem to exist three different ways for analyzing spatiotemporal signals. The first one, which has been extensively studied in the past, focuses on the temporal evolution of the signal. Here, the dynamics is characterized in terms of metric properties of the underlying attractors like Lyapunov exponents and fractal dimensions [8]. On the other hand, great efforts have been made in reconstructing the dynamics by introducing time-delay coordinates [9] or principal component analysis (with respect to the temporal evolution) [10]. Furthermore, attempts have been made to fit sets of ordinary differential equations to the experimentally obtained time series [11,12]. Yet there are still open questions concerning the applicability, reliability, and significance of these techniques [13–15].

A second approach concentrates on the spatial features of a signal, with the aim of finding a mode expansion converging best with respect to the least-square deviation, by applying principal component analysis (compare Sec. III B and e.g., [1,16]). In case where the evolution equation of the system under consideration is known, as e.g., for hydrodynamic problems, it is possible to obtain finite dimensional Galerkin approximations to the dynamics by projecting the evolution equations onto the modes obtained by the principal component analysis.

A third approach has been discussed by us in a previous paper [17]. Here, we restrict our attention to the class of complex systems that are close to nonequilibrium phase transitions where the behavior changes qualitatively. These systems are studied in the field of synergetics [18,19], and it is well known that the spatiotemporal signal of such systems can then be described by a finite number of order parameters, which are amplitudes of spatial modes, and stable modes, whose amplitudes are determined by the other parameters. The dynamical evolution of the system is entirely governed by the dynamics of the order parameters which obey a finite dimensional set of ordinary differential equations. The natural way to analyze spatiotemporal signals of such systems, therefore, consists in identifying the order parameters of the system and determining the dynamical system governing their evolution.

A presentation of our method as well as its applications to instabilities with low codimension is the topic of the present paper. It is organized as follows. In Sec. II we briefly sketch the mathematical representation of the state vector of complex systems close to instabilities in terms of order parameters, unstable and stable modes. Then we present an outline of the general procedure of our algorithm. In Sec. IV we treat various types of codimension-I and -II bifurcations. Finally, we analyze spatiotemporal patterns, the so-called blinking states, which have been calculated from a partial differential equation modeling the oscillatory instability towards traveling waves of a spatially homogeneous state in large but finite quasi-one-dimensional systems.

II. SYSTEMS CONSIDERED

Spatiotemporal patterns may emerge in self-organizing complex systems exhibiting qualitative changes of its macroscopic behavior near instabilities [18,19]. The mathematical structures underlying these processes of spontaneous pattern formation are well understood. In the following we shall summarize the main characteristics.

The state vector $\tilde{\mathbf{q}}(t)$, which describes the pattern forming system, is assumed to obey a nonlinear evolution equation,

$$\dot{\tilde{\mathbf{q}}} = \mathbf{N}(\{\epsilon\}, \tilde{\mathbf{q}}) , \tag{1}$$

with $\{\epsilon\}$ being a set of control parameters. Close to instability the state vector $\tilde{\mathbf{q}}$ can be represented as a superposition of unstable ($\tilde{\mathbf{u}}$) and stable modes ($\tilde{\mathbf{s}}$) according to

$$\tilde{\mathbf{q}}(t)=\sum_u \xi_u(t)\tilde{\mathbf{u}}+\sum_s \xi_s(t)\tilde{\mathbf{s}}\ , \tag{2}$$

where $\tilde{\mathbf{u}}$ and $\tilde{\mathbf{s}}$ may be space-dependent vector functions. It is a well-established fact that close to instability the dynamics of the amplitudes of the stable modes $\xi_s(t)$ is determined entirely by the amplitudes $\xi_u(t)$ of the unstable modes after transient behavior has died away: the amplitudes of the stable modes $\xi_s(t)$ are "enslaved" by the order parameters $\xi_u(t)$ of the system. In mathematical terms, the amplitudes $\xi_s(t)$ move on a center manifold obeying an equation of the form

$$\begin{aligned}\xi_s(t)&=f_s[\{\xi_u(t)\}]\\&=\sum_{u,u'} k^{(2)}_{suu'}\xi_u\xi_{u'}+\sum_{u,u',u''} k^{(3)}_{suu'u''}\xi_u\xi_{u'}\xi_{u''}+\cdots\ .\end{aligned} \tag{3}$$

As a result the temporal evolution of the order parameters is determined by a closed set of nonlinear order parameter equations,

$$\begin{aligned}\dot{\xi}_u&=f_u[\{\epsilon\},\{\xi_u\}]\\&=a^{(0)}_u+a^{(1)}_u\xi_u+\sum_{u',u''} a^{(2)}_{uu'u''}\xi_{u'}\xi_{u''}\\&\quad+\sum_{u',u'',u'''} a^{(3)}_{uu'u''u'''}\xi_{u'}\xi_{u''}\xi_{u'''}+\cdots\ .\end{aligned} \tag{4}$$

Thus a pattern forming system allows for two levels of description. The microscopic level is determined by the basic evolution law (1). The macroscopic description is based on the representation (2) as well as on the order parameter equation (4). This forms the theoretical scheme of the description of the state vector of a pattern forming system close to instability.

It is immediately evident that a macroscopic analysis of spatiotemporal patterns of this class of systems should aim at a determination of order parameters and enslaved modes. To achieve this, one has to simultaneously determine the spatial modes $\tilde{\mathbf{u}},\tilde{\mathbf{s}}$ as well as their dynamical evolution, i.e., the coefficients of Eqs. (3) and (4). This will be described in the next section.

To conclude this section we remind the reader that the above outlined framework of the description of a pattern forming system is valid for systems close to instabilities, but recent results on the existence of inertial manifolds shows that it may also hold for more general situations. Our method of analysis also applies to these cases.

III. PROCEDURE

A. The number of order parameters and their dynamics

In order to apply our procedure to spatiotemporal signals one first has to specify the number of order parameters. Presently, we are not able to indicate a way to extract this number from the signals. In the present paper, we assume that the character of the instability is known so that the number of order parameters is fixed. The dynamical system of the order parameters can then be established in the following way. Since the system is close to an instability, nonlinearities are weak and may be approximated by polynomial expressions. Furthermore, symmetry considerations as well as normal form arguments may help to restrict the number of polynomial terms. In general, one has to start making guesses about the number of order parameters that has then to be confirmed self-consistently.

B. Projection into the relevant subspace

Our starting point is a given trajectory $\tilde{\mathbf{q}}(t)$ in an n-dimensional space Γ_n. The vector components $\tilde{q}_i(t)$ can either represent the spatial dependence of a spatiotemporal signal $\tilde{q}(\mathbf{x}_i,t)$ with discretized space elements $\mathbf{x}_i$, or other experimentally accessible quantities. Since the trajectory $\tilde{\mathbf{q}}(t)$ may move in a subspace $\Gamma_m\subseteq\Gamma_n$, it will be sufficient to analyze the signal in Γ_m, i.e., to project $\tilde{\mathbf{q}}(t)\in\Gamma_n$ into Γ_m calling the resulting trajectory $\mathbf{q}(t)$.

One way of detecting the relevant subspace Γ_m is given by the principal component analysis (PCA, also known as Karhunen-Loève decomposition, see e.g., [1,16]). To accomplish this one has to solve the eigenvalue problem,

$$C\mathbf{v}_j=\lambda_j\mathbf{v}_j\ , \tag{5}$$

of the correlation matrix C

$$C_{ij}=\langle\tilde{q}_i\tilde{q}_j\rangle:=\frac{1}{T}\int_{t_0}^{t_0+T}\tilde{q}_i(t)\tilde{q}_j(t)dt\ . \tag{6}$$

The eigenvectors $\mathbf{v}_j$ with nonneglectable eigenvalues λ_j span the subspace Γ_m. This restriction may simultaneously lead to a noise reduction of our signal.

Note that PCA is only a first and often dispensable step of our analysis which in particular aims at determining the adequate vectors in the subspace Γ_m. As it will turn out the resulting spatial modes in general differ strongly from the original PCA modes.

C. Parameter identification

The determination of the spatial modes and the coefficients of Eqs. (3) and (4) is achieved by means of an extremum principle. To this end we introduce a set of biorthogonal modes $\mathbf{s}^\dagger$, $\mathbf{u}^\dagger$, $\mathbf{s}$, and $\mathbf{u}$, which obey a relation of the form

$$\begin{aligned}&\mathbf{u}^\dagger\cdot\mathbf{u}'=\delta_{u,u'},\quad \mathbf{s}^\dagger\cdot\mathbf{u}=0\ ,\\&\mathbf{u}^\dagger\cdot\mathbf{s}=0,\quad \mathbf{s}^\dagger\cdot\mathbf{s}'=\delta_{s,s'}\ .\end{aligned} \tag{7}$$

The amplitudes $\xi_s(t)$ and $\xi_u(t)$ are, therefore, given by

$$\xi_s(t)=\mathbf{q}(t)\cdot\mathbf{s}^\dagger,\quad \xi_u(t)=\mathbf{q}(t)\cdot\mathbf{u}^\dagger\ . \tag{8}$$

Now we introduce the potential V as the mean square deviation of Eqs. (3) and (4),

$$V=\sum_s\frac{\langle(\xi_s-f_s[\{\xi_u\}])^2\rangle}{\langle\xi_s^2\rangle}+\sum_u\frac{\langle(\dot{\xi}_u-f_u[\{\xi_u\}])^2\rangle}{\langle\dot{\xi}_u^2\rangle}\ , \tag{9}$$

The denominators guarantee an equally weighted contribution of every term of the sum to the potential. Inserting Eqs. (3), (4), and (7) into Eq. (9) one obtains a potential V,

$$V=V[\{\mathbf{u}^\dagger\},\{\mathbf{s}^\dagger\},\{k^{(2)}_{su'u''}\},\ldots,\{a^{(0)}_u\},\{a^{(1)}_u\},\{a^{(2)}_{uu'u''}\},\ldots]+(\text{constraints}) , \tag{10}$$

depending on the biorthogonal modes $\mathbf{u}^\dagger,\mathbf{s}^\dagger$ and the coefficients of the center manifold $\{k\}$ and the order parameter equation $\{a\}$. The minimum of this potential yields our desired description of the spatiotemporal signal in terms of order parameters, enslaved modes and the corresponding spatial patterns.

In general the potential (10) is rather high dimensional and a straightforward search for the minimum is practically very difficult. However, the following observation allows a reduction of the unknown variables. The coefficients of the dynamics, $\{k\},\{a\}$, as well as the spatial modes $\mathbf{s}^\dagger$ occur only up to the power of 2 in the potential V, and therefore, the minimum of V with respect to these parameters can be obtained analytically as a function of the modes $\mathbf{u}^\dagger$ (for mathematical details we refer the reader to the Appendix). Inserting these minimal values into our potential yields a nonlinear function depending solely on the unstable modes

$$V=V[\{\mathbf{u}^\dagger\}] . \tag{11}$$

The minimum of this function, which can be found by gradient dynamics, represents the best choice of parameters for the assumed type of instability.

In the following we present the four generic cases of codimension-1 instabilities, a codimension-2 instability with reflection symmetry, and the application of the algorithm to a simulated spatiotemporal signal of a problem of fluid dynamics, simulated by integrating a partial differential equation.

IV. EXAMPLES

A. Steady-state bifurcations

In these cases there exists only one order parameter ξ_u with three typical types of bifurcations, the saddle-node bifurcation with normal form

$$\dot{\xi}_u=\epsilon\pm\xi_u^2 , \tag{12}$$

the transcritical bifurcation with normal form

$$\dot{\xi}_u=\epsilon\xi_u\pm\xi_u^2 \tag{13}$$

and the pitchfork bifurcation with normal form

$$\dot{\xi}_u=\epsilon\xi_u\pm\xi_u^3 . \tag{14}$$

As an example we assume one stable mode $\mathbf{s}$ with its amplitude $\xi_s(t)$,

$$\xi_s(t)=k\xi_u^2(t) , \tag{15}$$

neglecting as a first approximation terms of higher order than ξ_u^2.

The least-square-fit potential, taking all three bifurcations into account, is given by

$$V(\{a_i\},k,\mathbf{s}^\dagger,\mathbf{u}^\dagger)=\frac{\langle(\xi_s-k\xi_u^2)^2\rangle}{\langle\xi_s^2\rangle}+\frac{\langle(\dot{\xi}_u-a_0-a_1\xi_u-a_2\xi_u^2-a_3\xi_u^3)^2\rangle}{\langle\dot{\xi}_u^2\rangle} ,$$

with

$$\xi_s=\mathbf{q}(t)\cdot\mathbf{s}^\dagger,\quad \xi_u=\mathbf{q}(t)\cdot\mathbf{u}^\dagger , \tag{16}$$

with $\mathbf{q}(t)$ being the spatiotemporal signal $\tilde{\mathbf{q}}(t)$ projected into the relevant subspace.

As constraints we define $\langle\xi_s^2\rangle=c_s$, which we include in the potential by a Lagrange parameter and $\langle\xi_u^2\rangle=c_u$, which is considered explicitly as a constraint concerning $\mathbf{u}^\dagger$.

Variation with respect to k and $\mathbf{s}^\dagger$ after elimination of the Lagrange parameter yields

$$\begin{aligned} k&=k(\mathbf{u}^\dagger)=\sqrt{c_s}\frac{[\Gamma_3\Gamma_2^{-1}\Gamma_3(:\mathbf{u}^\dagger)^4]^{1/2}}{\Gamma_4(:\mathbf{u}^\dagger)^4} ,\\ \mathbf{s}^\dagger&=\mathbf{s}^\dagger(\mathbf{u}^\dagger)=\sqrt{c_s}\frac{\Gamma_2^{-1}\Gamma_3(:\mathbf{u}^\dagger)^2}{[\Gamma_3\Gamma_2^{-1}\Gamma_3(:\mathbf{u}^\dagger)^4]^{1/2}} . \end{aligned} \tag{17}$$

We thereby introduced symmetric correlation tensors Γ_2, Γ_3, and Γ_4,

$$\begin{aligned} &(\Gamma_2)_{ij}=\langle q_iq_j\rangle,\quad (\Gamma_3)_{ijk}=\langle q_iq_jq_k\rangle ,\\ &(\Gamma_4)_{ijkl}=\langle q_iq_jq_kq_l\rangle , \end{aligned} \tag{18}$$

and abbreviations such as

$$\Gamma_4(:\mathbf{u}^\dagger)^4=\sum_{ijkl}(\Gamma_4)_{ijkl}u_i^\dagger u_j^\dagger u_k^\dagger u_l^\dagger ,$$

$$\Gamma_3\Gamma_2^{-1}\Gamma_3(:\mathbf{u}^\dagger)^4=\sum_{ijklmn}(\Gamma_3)_{ijk}(\Gamma_2^{-1})_{kl}(\Gamma_3)_{lmn}u_i^\dagger u_j^\dagger u_m^\dagger u_n^\dagger .$$

The inverse Γ_2^{-1} of the correlation matrix Γ_2 exists, since $\mathbf{q}(t)$ is the trajectory of $\tilde{\mathbf{q}}(t)$ projected into the relevant subspace.

By variation with respect to the coefficients $\{a_i\}$ we obtain

$$\begin{bmatrix}a_0\\a_1\\a_2\\a_3\end{bmatrix}=\begin{bmatrix}1&\langle\xi_u\rangle&\langle\xi_u^2\rangle&\langle\xi_u^3\rangle\\ \langle\xi_u\rangle&\langle\xi_u^2\rangle&\langle\xi_u^3\rangle&\langle\xi_u^4\rangle\\ \langle\xi_u^2\rangle&\langle\xi_u^3\rangle&\langle\xi_u^4\rangle&\langle\xi_u^5\rangle\\ \langle\xi_u^3\rangle&\langle\xi_u^4\rangle&\langle\xi_u^5\rangle&\langle\xi_u^6\rangle\end{bmatrix}^{-1}\begin{bmatrix}\langle\dot{\xi}_u\rangle\\ \langle\dot{\xi}_u\xi_u\rangle\\ \langle\dot{\xi}_u\xi_u^2\rangle\\ \langle\dot{\xi}_u\xi_u^3\rangle\end{bmatrix} , \tag{19}$$

which again can be written as a function of $\mathbf{u}^\dagger$, whereby correlation tensors Γ_i up to the sixth order and correlation tensors Λ_i,

$$(\Lambda_1)_i=\langle \dot{q}_i \rangle, \quad (\Lambda_2)_{ij}=\langle \dot{q}_i q_j \rangle ,$$
$$(\Lambda_3)_{ijk}=\langle \dot{q}_i q_j q_k \rangle, \ldots \tag{20}$$

occur.

By inserting Eqs. (17) and (19) into the potential V [Eq. (16)] we obtain a nonlinear potential $V(\mathbf{u}^\dagger)$ depending only on $\mathbf{u}^\dagger$

$$V(\mathbf{u}^\dagger)=V_s(\mathbf{u}^\dagger)+V_u(\mathbf{u}^\dagger) ,$$
$$V_s(\mathbf{u}^\dagger)=1-\frac{\Gamma_3\Gamma_2^{-1}\Gamma_3(:\mathbf{u}^\dagger)^4}{\Gamma_4(:\mathbf{u}^\dagger)^4} ,$$
$$V_u(\mathbf{u}^\dagger)=1-\frac{1}{\Delta_2(:\mathbf{u}^\dagger)^2}M^{-1}[\mathbf{u}^\dagger](:\mathbf{y}[\mathbf{u}^\dagger])^2 , \tag{21}$$

with

$$(\Delta_2)_{ij}=\langle \dot{q}_i \dot{q}_j \rangle$$
$$\mathbf{y}[\mathbf{u}^\dagger]=(\Lambda_1(:\mathbf{u}^\dagger),\Lambda_2(:\mathbf{u}^\dagger)^2,\Lambda_3(:\mathbf{u}^\dagger)^3,\Lambda_4(:\mathbf{u}^\dagger)^4)^T$$

$$M[\mathbf{u}^\dagger]=\begin{bmatrix} 1 & \Gamma_1(:\mathbf{u}^\dagger) & \Gamma_2(:\mathbf{u}^\dagger)^2 & \Gamma_3(:\mathbf{u}^\dagger)^3 \\ \Gamma_1(:\mathbf{u}^\dagger) & \Gamma_2(:\mathbf{u}^\dagger)^2 & \Gamma_3(:\mathbf{u}^\dagger)^3 & \Gamma_4(:\mathbf{u}^\dagger)^4 \\ \Gamma_2(:\mathbf{u}^\dagger)^2 & \Gamma_3(:\mathbf{u}^\dagger)^3 & \Gamma_4(:\mathbf{u}^\dagger)^4 & \Gamma_5(:\mathbf{u}^\dagger)^5 \\ \Gamma_3(:\mathbf{u}^\dagger)^3 & \Gamma_4(:\mathbf{u}^\dagger)^4 & \Gamma_5(:\mathbf{u}^\dagger)^5 & \Gamma_6(:\mathbf{u}^\dagger)^6 \end{bmatrix} . \tag{22}$$

If the signal $\tilde{\mathbf{q}}(t)$ consists of two modes $\tilde{\mathbf{u}}$ and $\tilde{\mathbf{s}}$ the subspace is two dimensional. $\mathbf{u}^\dagger$ can then be written as a vector with two components,

$$\mathbf{u}^\dagger=\begin{bmatrix} x_1 \\ x_2 \end{bmatrix} , \tag{23}$$

which has to fulfill the constraint

$$\langle \xi_u^2 \rangle=\langle [\mathbf{q}(t)\mathbf{u}^\dagger]^2 \rangle$$
$$=\langle q_1^2 \rangle x_1^2+2\langle q_1 q_2 \rangle x_1 x_2+\langle q_2^2 \rangle x_2^2=c_u . \tag{24}$$

If the signal $\tilde{\mathbf{q}}(t)$ was projected using PCA, $\langle q_i q_j \rangle$ is given by

$$\langle q_i q_j \rangle=\lambda_i \delta_{ij} , \tag{25}$$

with λ_i being the eigenvalues of Eq. (5). Equation (24) then describes the normal form of an ellipse in the plane. We can introduce polar coordinates and obtain

$$\mathbf{u}^\dagger=\begin{bmatrix} r_1\cos\phi \\ r_2\sin\phi \end{bmatrix}, \quad r_1=[c_u/\lambda_1]^{1/2} ,$$
$$r_2=[c_u/\lambda_2]^{1/2} . \tag{26}$$

The potential V [Eq. (21)] now depends only on one parameter, the angle ϕ

$$V(\phi)=V_s(\phi)+V_u(\phi) , \tag{27}$$

with a translational symmetry $V(\phi)=V(\phi+\pi)$, due to the still possible scaling of $\mathbf{u}^\dagger$ with -1.

Figure 1 shows the potential $V(\phi)$ calculated from simulated spatiotemporal signals $\tilde{\mathbf{q}}(t)=\xi_u(t)\tilde{\mathbf{u}}+\xi_s(t)\tilde{\mathbf{s}}$. The amplitudes $\xi_u(t)$ and $\xi_s(t)$ were obtained by numerical integration of ordinary differential equations showing the three different types of normal forms [Eqs. (12), (13), and (14)] and a center manifold like Eq. (15). As spatial modes $\tilde{\mathbf{u}},\tilde{\mathbf{s}}$ we chose the modes shown in Fig. 2(a). The dashed line of Fig. 1 represents $V_u(\phi)$, the dotted $V_s(\phi)$ and the solid line the sum of them, $V=V_u+V_s$. In all three cases we obtain a distinct minimum of the potential V representing the right choice of parameters. The term $V_s(\phi)$ helps to avoid additional local minima, occurring in $V_u(\phi)$. They are due to the fact, that—besides ξ_u—a certain linear combination of ξ_u and ξ_s, $\xi=\alpha\xi_u+\beta\xi_s$, fulfills in a good approximation a differential equation of the form

$$\dot{\xi}=a_0+a_1\xi+a_2\xi^2+a_3\xi^3 . \tag{28}$$

For example, in Fig. 1(c) we plotted the potential $V=V_u+V_s$ of the Haken-Zwanzig model,

$$\dot{\xi}_s=-\xi_s+k\xi_u^2 ,$$
$$\dot{\xi}_u=\epsilon\xi_u+\gamma\xi_u\xi_s . \tag{29}$$

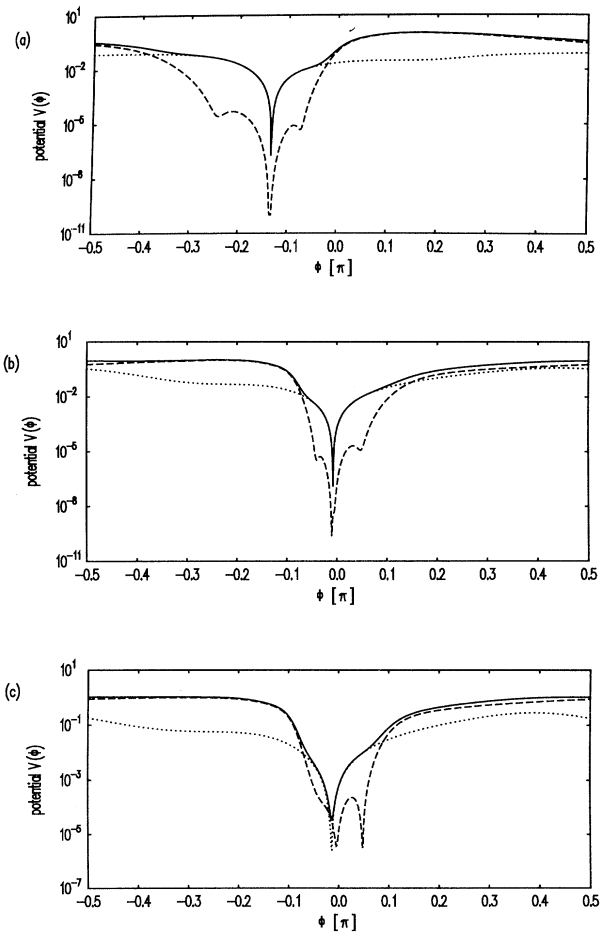

FIG. 1. Potential $V(\phi)$ (solid line), $V_u(\phi)$ (dashed line), and $V_s(\phi)$ (dotted line) for different simulated types of bifurcations: (a) saddle-node bifurcation, (b) transcritical bifurcation, and (c) pitchfork bifurcation.

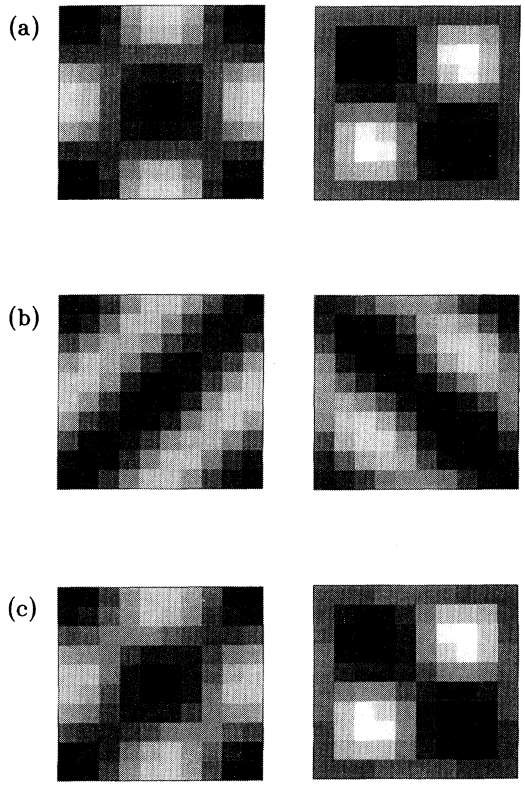

FIG. 2. (a) Simulated spatial modes $\tilde{\mathbf{u}}$ and $\tilde{\mathbf{s}}$, (b) the resulting two vectors of PCA, and (c) modes, obtained by our method.

There occur two deep minima of V_u (dashed line): one, coinciding with the minimum of V_s and, therefore, the searched one representing $\beta=0$, and an additional local minimum of V_u representing $\alpha=0$, since for $\alpha=0$, $\dot{\xi}\simeq\beta 2k\xi_u\dot{\xi}_u=\beta(2\epsilon\xi+2\gamma\xi^2)$ fulfills the differential equation (28) as well.

Figure 2(b) shows the two modes obtained by PCA, calculated from the simulated spatiotemporal signal of the Haken-Zwanzig model. The modes $\tilde{\mathbf{u}}$ and $\tilde{\mathbf{s}}$ obtained by our algorithm are presented in Fig. 2(c). They are in quite good correspondence with the modes of the simulated data [Fig. 2(a)]. That there is no perfect agreement is due to the ansatz of V_s and V_u. The Haken-Zwanzig model [Eq. (29)] yields a center manifold,

$$\xi_s=k(1-2\epsilon)\xi_u^2+O(\xi_u^4)\ , \tag{30}$$

and a order parameter equation,

$$\dot{\xi}_u=\epsilon\xi_u+\gamma k(1-2\epsilon)\xi_u^3+O(\xi_u^5)\ . \tag{31}$$

In our ansatz of V_s and V_u, we neglected the higher order terms $O(\ )$ as a first approximation, which is the first reason for not obtaining the exact modes. A second reason is given by the general ansatz of V_u: We do not assume a pitchfork bifurcation in advance, but minimize a more general ansatz. The minimum of this ansatz does not lead to an exact pitchfork bifurcation and, therefore, the exact modes are not obtained. However, the occurrence of the pitchfork bifurcation is detected very well and demonstrated by Fig. 3. There we show the dependence of the coefficients $a_i(\phi)$ again from the simulated data of the Haken-Zwanzig model. The dotted line indicates the minimum of the potential $V(\phi)$, the dashed line corresponds to $a_i=0$ and the little cross marks the value of $a_i(\phi)$ given by the coefficients of the integrated ordinary differential equation. The coefficients corresponding to the minimum are in good agreement with the model, especially the type of bifurcation is detected clearly: $a_0=a_2=0$ corresponds to the pitchfork bifurcation.

This example shows that our presented algorithm is able to classify the spatiotemporal signal into the right type of bifurcation and it yields a good choice of parame-

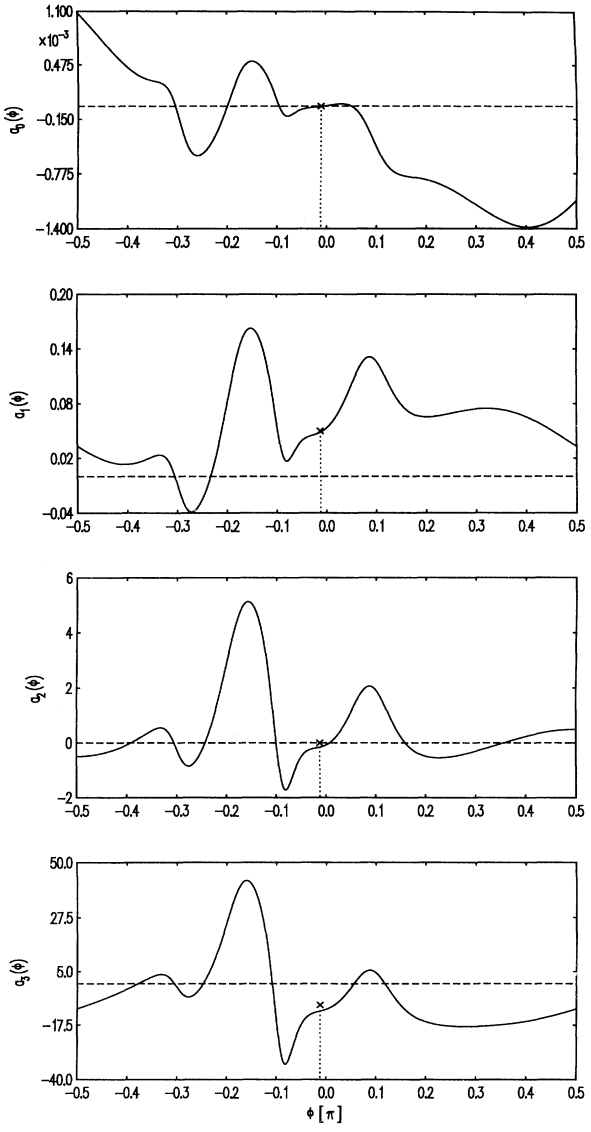

FIG. 3. Coefficients $a_i(\phi)$ of a simulated Haken-Zwanzig model. The dashed line represents $a_i=0$, the dotted line the minimum of the potential in Fig. 1(c). The little cross marks the coefficients of the simulation.

ters corresponding to the temporal evolution and the spatial modes of the signal. After detection of the type of bifurcation one can define a new least-square-fit potential V_u minimizing the deviation of the given normal form only, like described in [17], which then leads to the best choice of parameters corresponding to this specific normal form.

B. Hopf bifurcation

In the fourth case of a codimension-I instability, the Hopf bifurcation, there exist two order parameters obeying the normal form

$$\frac{d}{dt}\begin{bmatrix}\xi_1\\ \xi_2\end{bmatrix}=\begin{bmatrix}\epsilon & -\omega\\ \omega & \epsilon\end{bmatrix}\begin{bmatrix}\xi_1\\ \xi_2\end{bmatrix}+(\xi_1^2+\xi_2^2)\begin{bmatrix}a & -b\\ b & a\end{bmatrix}\begin{bmatrix}\xi_1\\ \xi_2\end{bmatrix}. \tag{32}$$

The transformation into a complex differential equation, introducing a complex variable, $c(t)=\xi_1(t)+i\xi_2(t)=r(t)\exp[i\phi(t)]$, yields

$$\dot{c}=\alpha c+\beta|c|^2c\ , \tag{33}$$

with

$$\alpha=\epsilon+i\omega,\quad \beta=a+ib\ . \tag{34}$$

The corresponding least-square-fit potential V_c then reads,

$$V_c=\frac{\langle|\dot{c}-\alpha c-\beta|c|^2c|^2\rangle}{\langle|\dot{c}|^2\rangle}\ . \tag{35}$$

Again as an example, we assume one stable mode $\mathbf{s}$, with an approximated center manifold,

$$\xi_s(t)=k|c(t)|^2\ . \tag{36}$$

The least-square-fit potential V for this scenario, rewritten in polar coordinates, is then given by

$$\begin{aligned}V&=V_s+V_r+V_\phi\ ,\\ V_s&=\frac{\langle(\xi_s-kr^2)^2\rangle}{\langle\xi_s^2\rangle}\ ,\\ V_r&=\frac{\langle(\dot{r}-\epsilon r-ar^3)^2\rangle}{\langle\dot{r}^2\rangle+\langle r^2\dot{\phi}^2\rangle}\ ,\\ V_\phi&=\frac{\langle(r\dot{\phi}-\omega r-br^3)^2\rangle}{\langle\dot{r}^2\rangle+\langle r^2\dot{\phi}^2\rangle}\ .\end{aligned} \tag{37}$$

As constraints to fix scaling and rotation of $\mathbf{u}_1^\dagger,\mathbf{u}_2^\dagger$, we require $\langle r^2\rangle=c_r$ and $\xi_1(t_0)=0$, and as a constraint concerning $\mathbf{s}^\dagger$ we choose $\langle\xi_s^2\rangle=c_s$, which again is taken care of by a Lagrange parameter.

By variation with respect to $\mathbf{s}^\dagger$, k, ϵ, ω, a, and b we obtain these parameters as a function of $\mathbf{u}_1^\dagger$, $\mathbf{u}_2^\dagger$. Inserting them into Eq. (37) yields a nonlinear potential V depending on $\mathbf{u}_1^\dagger,\mathbf{u}_2^\dagger$ only

$$\begin{aligned}V(\mathbf{u}_1^\dagger,\mathbf{u}_2^\dagger)&=V_s(\mathbf{u}_1^\dagger,\mathbf{u}_2^\dagger)+V_r(\mathbf{u}_1^\dagger,\mathbf{u}_2^\dagger)+V_\phi(\mathbf{u}_1^\dagger,\mathbf{u}_2^\dagger)\ ,\\ V_s(\mathbf{u}_1^\dagger,\mathbf{u}_2^\dagger)&=1-\frac{\Gamma_3\Gamma_2^{-1}\Gamma_3((:\mathbf{u}_1^\dagger)^2+(:\mathbf{u}_2^\dagger)^2)^2}{\Gamma_4((:\mathbf{u}_1^\dagger)^2+(:\mathbf{u}_2^\dagger)^2)^2}\ ,\end{aligned} \tag{38}$$

$$V_r(\mathbf{u}_1^\dagger,\mathbf{u}_2^\dagger)+V_\phi(\mathbf{u}_1^\dagger,\mathbf{u}_2^\dagger)=1-\frac{1}{\langle\dot{r}^2+r^2\dot{\phi}^2\rangle}\times M_H^{-1}((:\mathbf{y}_1)^2+(:\mathbf{y}_2)^2)\ ,$$

with

$$M_H=\begin{bmatrix}\langle r^2\rangle & \langle r^4\rangle\\ \langle r^4\rangle & \langle r^6\rangle\end{bmatrix},\quad \mathbf{y}_1=\begin{bmatrix}\langle r\dot{r}\rangle\\ \langle r^3\dot{r}\rangle\end{bmatrix},\quad \mathbf{y}_2=\begin{bmatrix}\langle r^2\dot{\phi}\rangle\\ \langle r^4\dot{\phi}\rangle\end{bmatrix}. \tag{39}$$

The occurring correlations $\langle\ \rangle$ can all be written in terms of ξ_1 and ξ_2,

$$\begin{aligned}\langle r^2\rangle&=\langle\xi_1^2+\xi_2^2\rangle\ ,\\ \langle r^4\rangle&=\langle(\xi_1^2+\xi_2^2)^2\rangle\ ,\\ \langle r^6\rangle&=\langle(\xi_1^2+\xi_2^2)^3\rangle\ ,\\ \langle r\dot{r}\rangle&=\langle\xi_1\dot{\xi}_1+\xi_2\dot{\xi}_2\rangle\ ,\\ \langle r^3\dot{r}\rangle&=\langle(\xi_1^2+\xi_2^2)(\xi_1\dot{\xi}_1+\xi_2\dot{\xi}_2)\rangle\ ,\\ \langle r^2\dot{\phi}\rangle&=\langle\xi_1\dot{\xi}_2-\dot{\xi}_1\xi_2\rangle\ ,\\ \langle r^4\dot{\phi}\rangle&=\langle(\xi_1^2+\xi_2^2)(\xi_1\dot{\xi}_2-\dot{\xi}_1\xi_2)\rangle\ ,\end{aligned} \tag{40}$$

which all can be expressed in terms of correlation tensors and spatial modes $\mathbf{u}_1^\dagger$ and $\mathbf{u}_2^\dagger$.

We now still have to consider the constraints $\xi_1(t_0)=0$ and $\langle r^2\rangle=c_r$, which yield a further reduction of parameters: If the signal $\tilde{\mathbf{q}}(t)$ consists of three modes $\tilde{\mathbf{u}}_1$, $\tilde{\mathbf{u}}_2$, and $\tilde{\mathbf{s}}$ the subspace is three dimensional. $\mathbf{u}_i^\dagger$ can then be expressed as vectors with three components. Taking the two constraints concerning $\mathbf{u}_i$ into account one ends up with four independent variables, which again can be transformed by generalized polar coordinates leading to four angles $\phi_1,\ldots,\phi_4$ as independent variables. The resulting potential is, therefore, four dimensional,

$$V=V(\phi_1,\phi_2,\phi_3,\phi_4)\ . \tag{41}$$

To verify our calculations we have simulated a spatiotemporal signal by numerical integration of a system of differential equations showing the normal form like Eq. (32) and a center manifold like Eq. (36). We obtained the minimum of the four-dimensional potential by gradient dynamics, the resulting parameters agreed perfectly with the parameters of the simulation.

To visualize the potential we have as well simulated a spatiotemporal signal with the unstable modes $\tilde{\mathbf{u}}_1$ and $\tilde{\mathbf{u}}_2$ only: $\tilde{\mathbf{q}}(t)=\xi_1(t)\tilde{\mathbf{u}}_1+\xi_2(t)\tilde{\mathbf{u}}_2$. The phase portrait of the amplitudes of the simulated example is shown in Fig. 4(a). The trajectory starts near the fix point $\xi_1=\xi_2=0$ and moves into the limit cycle. The subspace of the trajectory $\tilde{\mathbf{q}}(t)$ is then two dimensional, the modes $\mathbf{u}_1^\dagger,\mathbf{u}_2^\dagger$ can be expressed as two-dimensional vectors

$$\mathbf{u}_1^\dagger=\begin{bmatrix}x_1\\y_1\end{bmatrix},\quad \mathbf{u}_2^\dagger=\begin{bmatrix}x_2\\y_2\end{bmatrix}. \tag{42}$$

To fulfill the first constraint, $\xi_1(t_0)=0$, we obtain

$$x_1=\gamma y_1,\quad \gamma=-\frac{q_2(t_0)}{q_1(t_0)}. \tag{43}$$

After introducing polar coordinates and considering Eq. (43), the second constraint $\langle r^2\rangle=c_r$, yields

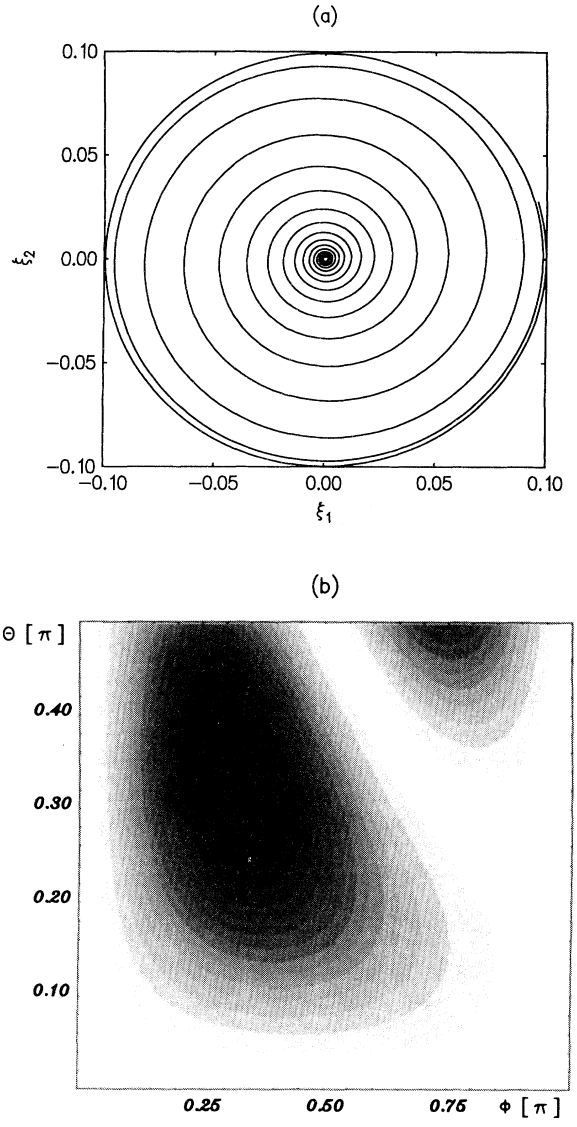

FIG. 4. (a) Phase portrait of the amplitudes $\xi_1(t)$ and $\xi_2(t)$ of a simulated super-critical Hopf bifurcation [Eq. (32), $\epsilon=0.05$, $\omega=1$, $a=-5$, and $b=75$]. (b) Two-dimensional least-square-fit potential $V_u(\phi,\theta)$ corresponding to the simulated Hopf bifurcation. The values of the potential $V(\phi,\theta)$ are given by different grey values: Black represents the minimum of the potential, white the maximum. The potential shows one distinct minimum and the expected symmetry $V(\phi-\pi/2,\theta=\pi/2)=V(\phi+\pi/2,\theta=\pi/2)$.

$$x_2=\left[\frac{c_r}{\lambda_1}\right]^{1/2}\cos\phi\sin\theta,$$
$$y_1=\left[\frac{c_r}{\gamma^2\lambda_1+\lambda_2}\right]^{1/2}\sin\phi\sin\theta, \tag{44}$$
$$y_2=\left[\frac{c_r}{\lambda_2}\right]^{1/2}\cos\theta,$$

with the eigenvalues λ_i of PCA. Thus the resulting potential is two dimensional depending only on two angles ϕ,θ. It shows the following reflection and translational symmetries:

$$V(\pi+\phi,\theta)=V(\pi-\phi,\theta),$$
$$V\left[\frac{\pi}{2}+\phi,\frac{\pi}{2}+\theta\right]=V\left[\frac{\pi}{2}-\phi,\frac{\pi}{2}-\theta\right], \tag{45}$$
$$V(\phi,\theta)=V(\phi,\theta+\pi),$$

due to the still possible scaling of $\mathbf{u}_1^\dagger,\mathbf{u}_2^\dagger$ or both with -1. Therefore, it is sufficient to search a minimum in the interval $0\le\phi\le\pi$ and $0\le\theta\le\pi/2$. Figure 4(b) shows the potential $V(\phi,\theta)$ of a simulated example showing a smooth function with no occurrence of any additional minima. The minimum represents, in perfect correspondence with the simulation, the coefficients of the dynamic evolution and the spatial modes.

C. A codimension-II instability

In the case of a codimension-II instability with reflection symmetry the normal form of the two occurring order parameters ξ_1,ξ_2 reads

$$\dot\xi_1=\xi_2$$
$$\dot\xi_2=\mu_1\xi_1+\mu_2\xi_2+c\xi_1^3-\xi_1^2\xi_2,\quad c=\pm1. \tag{46}$$

The least-square-fit potential V_u concerning the order parameters is then given by,

$$V_u=V_1+V_2,$$
$$V_1=\frac{\langle(\dot\xi_1-\tau\xi_2)^2\rangle}{\langle\dot\xi_1^2\rangle}, \tag{47}$$
$$V_2=\frac{\langle(\dot\xi_2-a\xi_1-b\xi_2-c\xi_1^3-d\xi_1^2\xi_2)^2\rangle}{\langle\dot\xi_2^2\rangle},$$

with two constraints fixing scaling,

$$\langle\xi_1^2\rangle=c_1,\quad \langle\xi_2^2\rangle=c_2. \tag{48}$$

The stable modes can be dealt with either by adding to V_u a potential V_s, in complete analogy to the previous cases, or by detecting them in a second step: In the first step one minimizes only V_u (with respect to $\mathbf{u}_i^\dagger$) and then one checks which of possible center manifolds occur by comparing the value of the minimum of V_s with respect to $\mathbf{s}^\dagger$ and fixed $\mathbf{u}_i^\dagger$.

Minimizing V_u with respect to the coefficients of the

temporal evolution and inserting them back into V_u, results in

$$V_1(\mathbf{u}_1^\dagger,\mathbf{u}_2^\dagger)=1-\frac{\langle\dot{\xi}_1\xi_2\rangle^2}{\langle\dot{\xi}_1^2\rangle\langle\xi_2^2\rangle},$$

$$V_2(\mathbf{u}_1^\dagger,\mathbf{u}_2^\dagger)=1-\frac{1}{\langle\dot{\xi}_2^2\rangle}M^{-1}[\mathbf{u}_1^\dagger,\mathbf{u}_2^\dagger](:\mathbf{y}[\mathbf{u}_1^\dagger,\mathbf{u}_2^\dagger])^2, \quad (49)$$

with

$$\mathbf{y}[\mathbf{u}_1^\dagger,\mathbf{u}_2^\dagger]=(\langle\dot{\xi}_2\xi_1\rangle,\langle\dot{\xi}_2\xi_2\rangle,\langle\dot{\xi}_2\xi_1^3\rangle,\langle\dot{\xi}_2\xi_1^2\xi_2\rangle)^T \quad (50)$$

and

$$M[\mathbf{u}_1^\dagger,\mathbf{u}_2^\dagger]=\begin{bmatrix}\langle\xi_1^2\rangle & \langle\xi_1\xi_2\rangle & \langle\xi_1^4\rangle & \langle\xi_1^3\xi_2\rangle\\ \langle\xi_1\xi_2\rangle & \langle\xi_2^2\rangle & \langle\xi_1^3\xi_2\rangle & \langle\xi_1^2\xi_2^2\rangle\\ \langle\xi_1^4\rangle & \langle\xi_1^3\xi_2\rangle & \langle\xi_1^6\rangle & \langle\xi_1^5\xi_2\rangle\\ \langle\xi_1^3\xi_2\rangle & \langle\xi_1^2\xi_2^2\rangle & \langle\xi_1^5\xi_2\rangle & \langle\xi_1^4\xi_2^2\rangle\end{bmatrix}. \quad (51)$$

Again, all occurring expressions can be written in terms of correlation tensors $\Gamma_i,\Lambda_i,\Delta_i$ and spatial modes $\mathbf{u}_1^\dagger,\mathbf{u}_2^\dagger$. Searching the minimum of V_u with respect to $\mathbf{u}_1^\dagger$ and $\mathbf{u}_2^\dagger$, one has to ensure that $u_1^\dagger$ and $u_2^\dagger$ are linearly independent, if not the matrix M cannot be inverted.

For the purpose of visualization of the potential $V_u(u_1^\dagger,\mathbf{u}_2^\dagger)$, we simulated a spatiotemporal signal $\tilde{\mathbf{q}}(t)=\xi_1(t)\tilde{\mathbf{u}}_1+\xi_2(t)\tilde{\mathbf{u}}_2$, by integrating Eq. (46) and assuming two spatial modes $\tilde{\mathbf{u}}_1,\tilde{\mathbf{u}}_2$. Figure 5(a) shows the trajectory in phase space of an example in which there exist two unstable foci and a saddle point, the trajectory moving into a limit cycle.

Because of the two-dimensional subspace the two spatial modes $\mathbf{u}_1^\dagger,\mathbf{u}_2^\dagger$ are two dimensional and can be written in polar coordinates fulfilling the constraints, $\langle\xi_1^2\rangle=c_1$, $\langle\xi_2^2\rangle=c_2$

$$\mathbf{u}_1^\dagger=\sqrt{c_1}\begin{bmatrix}\lambda_1^{-1/2}\cos\phi\\ \lambda_2^{-1/2}\sin\phi\end{bmatrix}\quad \mathbf{u}_2^\dagger=\sqrt{c_2}\begin{bmatrix}\lambda_1^{-1/2}\cos\theta\\ \lambda_2^{-1/2}\sin\theta\end{bmatrix}. \quad (52)$$

Therefore, the potential V_u depends only on two free parameters ϕ,θ, again with translational symmetry

$$V_u(\phi,\theta)=V_u(\phi+\pi,\theta)=V_u(\phi,\theta+\pi). \quad (53)$$

Figure 5(b) shows the potential $V_u(\phi,\theta)$ of the simulated example, a smooth function with one distinct local minimum representing, in perfect agreement with the simulation, all parameters of the temporal evolution and spatial modes.

D. Blinking states

In this example we would like to demonstrate the application of our algorithm to a spatiotemporal signal obtained by numerical integration of a partial differential equation, the so-called "blinking state." It has been experimentally observed in convection of binary mixtures [20] and can be modeled [21] by a generalized Ginzburg-Landau equation for a complex order parameter field $\Psi(x,t)$

$$\dot{\Psi}(x,t)=[\epsilon+i\omega_c-i\alpha(1+\partial_x^2)-(1+\partial_x^2)^2-|\Psi(x,t)|^2]\Psi(x,t). \quad (54)$$

Figure 6(a) shows the real part of the spatiotemporal signal, $\mathrm{Re}(\Psi(x,t))$, obtained by numerical integration of (54) considering boundary conditions,

$$\Psi(x_0,t)=\partial_x\Psi(x_0,t)=0,\quad x_0=0,\Gamma, \quad (55)$$

and parameter values $\epsilon=0.1$, $\alpha=0.4$, $\omega_c=3\alpha$, and $\Gamma=31$ (with a spatial discretization of 50 points). A theoretical analysis [21] of the model yields two linear unstable modes, $u_1(x)$ and $u_2(x)$, with different parity, which

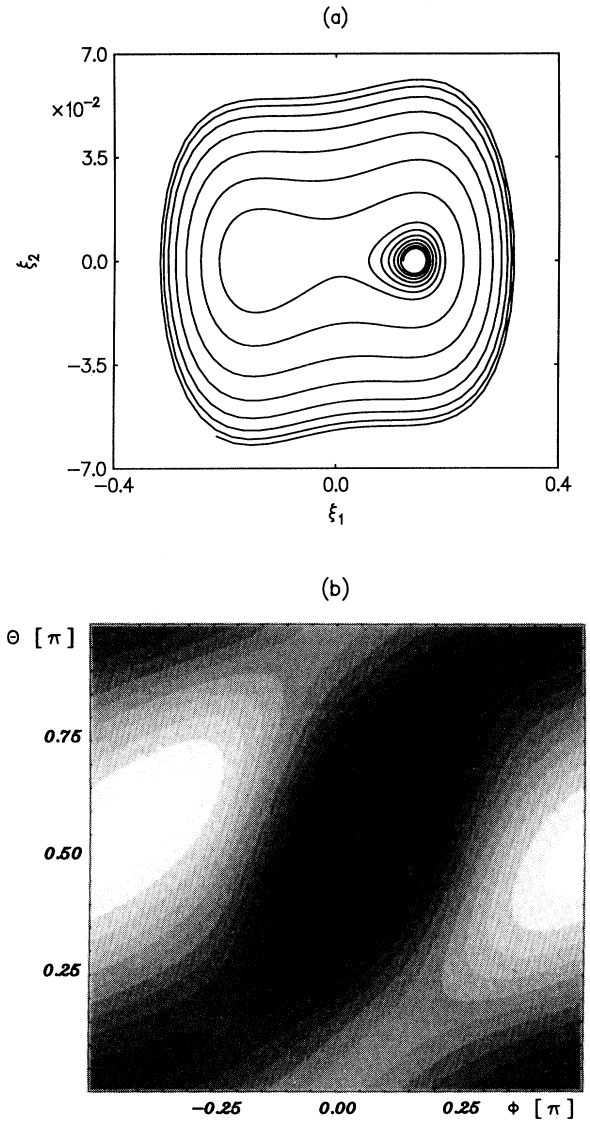

FIG. 5. (a) Phase portrait of the amplitudes $\xi_1(t)$ and $\xi_2(t)$ of a simulated codimension-two bifurcation [Eq. (46), $\mu_1=0.02$, $\mu_2=0.03$, $c=-1$]. (b) Least-square-fit potential $V_u(\phi,\theta)$ corresponding to the simulated codimension-two bifurcation with the same color coding as in Fig. 4(b). There occurs again one distinct minimum and the expected symmetry of a torus.

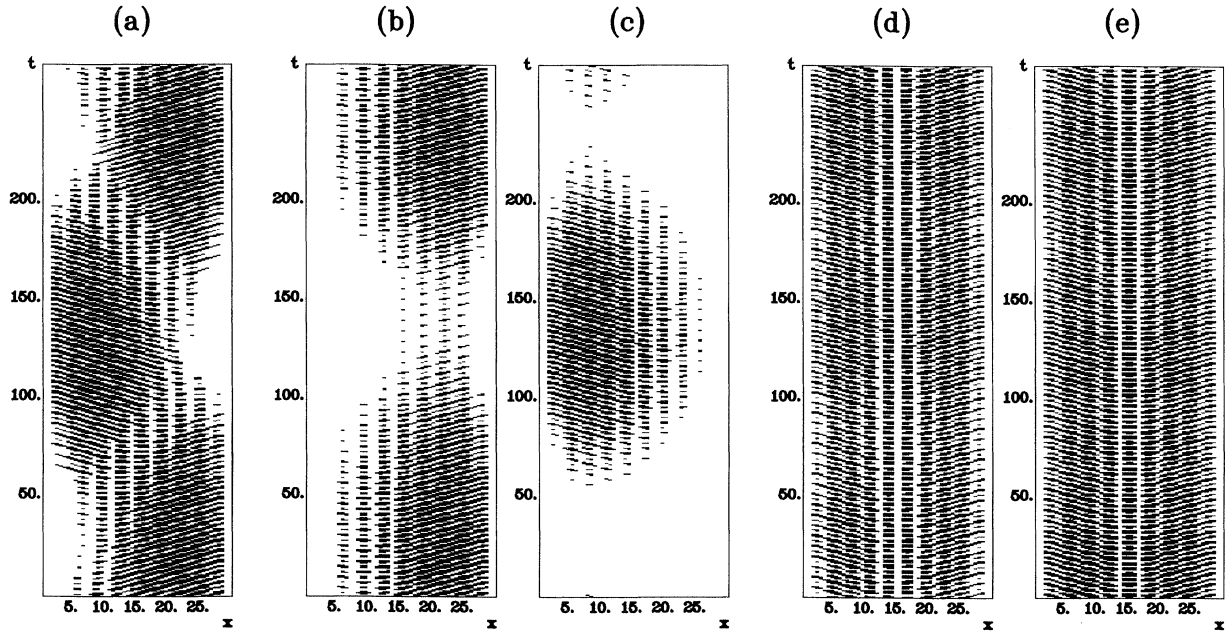

FIG. 6. (a) $\mathrm{Re}[\Psi(x,t)]$, obtained by integration of Eq. (54), (b) $\mathrm{Re}(\eta_1(t)v_1(x))$, (c) $\mathrm{Re}(\eta_2(t)v_2(x))$, both obtained by PCA of the signal $\Psi(x,t)$, (d) $\mathrm{Re}(\xi_1(t)u_1(x))$, and (e) $\mathrm{Re}(\xi_2(t)u_2(x))$, both obtained by the presented method.

govern the dynamics of the system,

$$\Psi(x,t)=\xi_1(t)u_1(x)+\xi_2(t)u_2(x)+O(\xi_u^3)\ . \tag{56}$$

The dynamics of the amplitudes of the unstable modes can be expressed in terms of ordinary differential equations,

$$\begin{aligned}\dot{\xi}_1(t)&=[\lambda_1-a_{11}|\xi_1(t)|^2-a_{12}|\xi_2(t)|^2]\xi_1(t)\\&\quad-b_1\xi_2^2(t)\xi_1^*(t)+O(\xi_u^5)\ ,\\\dot{\xi}_2(t)&=[\lambda_2-a_{21}|\xi_1(t)|^2-a_{22}|\xi_2(t)|^2]\xi_2(t)\\&\quad-b_2\xi_1^2(t)\xi_2^*(t)+O(\xi_u^5)\ ,\end{aligned} \tag{57}$$

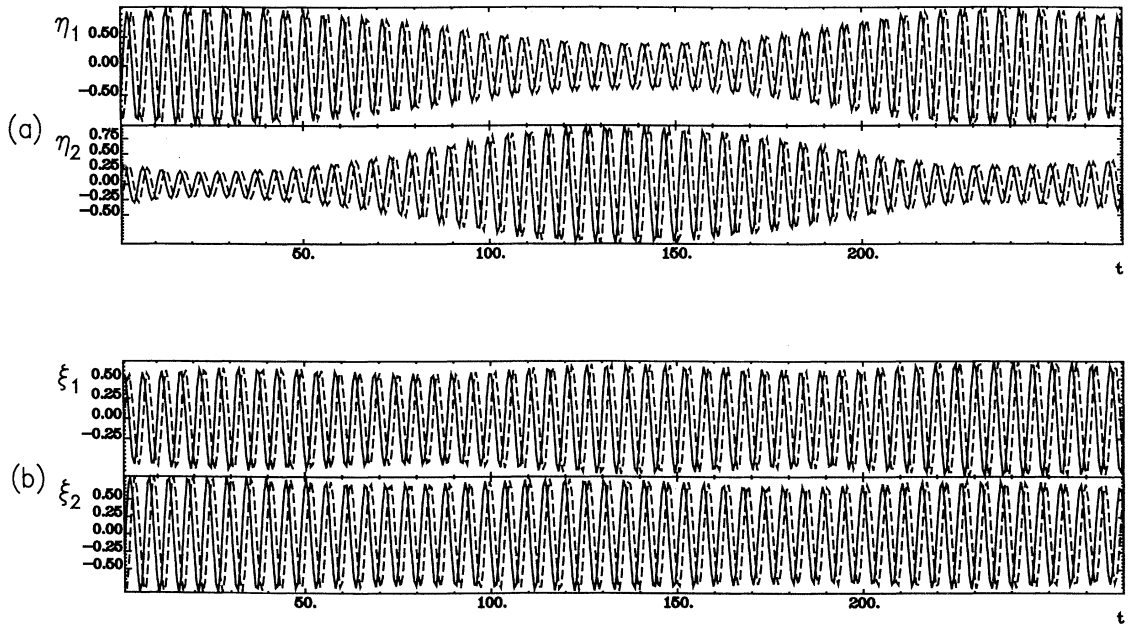

FIG. 7. (a) $\eta_1(t)$ and $\eta_2(t)$, both corresponding to the PCA modes of the signal $\Psi(x,t)$, (b) $\xi_1(t)$ and $\xi_2(t)$, both corresponding to the modes obtained by the presented method (solid line corresponds to the real part, dashed line to the imaginary part).

which correspond in the case of the blinking state to a quasiperiodic mode interaction.

Analyzing the simulated spatiotemporal signal $\Psi(x,t)$ with PCA yields two dominant complex modes, $v_1(x), v_2(x)$. The corresponding complex amplitudes, $\eta_1(t), \eta_2(t)$ are shown in Fig. 7(a). The contribution of the PCA modes to the signal is shown in Figs. 6(b) and 6(c). There is no symmetry of the modes recognizable, and the PCA modes do not correspond to the theoretical modes, and therefore, do not lead to the simple order parameter equations [Eqs. (57)].

Application of the presented algorithm, by introducing a least-square-fit potential considering the order parameter equations (57), one obtains complex spatial modes corresponding to the unstable modes, $u_1(x), u_2(x)$. Figure 7(b) shows the corresponding amplitudes, $\xi_1(t)$ and $\xi_2(t)$, and Figs. 6(d) and 6(c) presents the contribution of these modes to the signal. Clearly the symmetry of the modes can be recognized and the effect of the different time-depending phases of the amplitudes then leads to the spatiotemporal signal [Fig. 6(a)].

Summarizing this example, we would like to clarify similarities and differences between PCA and our presented method. Both, PCA and the presented method, yield the same spatiotemporal signal, but there are two big differences between these two approaches: First, symmetries of the modes can be lost by PCA, like this example clearly demonstrates. And second, an advantage of our presented method concerns the reconstruction of the signal by integrating ordinary differential equations. The number of coefficients that have to be calculated numerically from the signal, are much smaller with our algorithm than in the case of PCA. Both points are due to the fact that we minimize a least-square-error function of assumed order parameter equations, leading to a simultaneous search of dynamically and spatially relevant parameters, whereas PCA represents the search of a best converging mode expansion, without considering symmetries, underlying normal forms or the underlying dynamics.

V. CONCLUSIONS

We have derived a method for the determination of order parameters and corresponding center manifolds in spatiotemporal signals. It should be a helpful tool to analyze experimental data emerging from nonlinear self-organizing systems near instabilities. The occurring mode interaction in the vicinity of the critical points can be determined by the presented extremum principle. An advantage of the presented algorithm results from the simultaneous determination of spatial modes and parameters describing the temporal evolution. Our method yields nonlinear equations with the occurrence of higher order correlation tensors both of the signal and the time derivative of the signal. In this respect it represents an alternative to PCA and similar approaches, like [22], where spatial modes are obtained out of linear equations and second order correlation tensors.

ACKNOWLEDGMENTS

We gratefully acknowledge support and helpful discussions with M. Bestehorn concerning the blinking states.

APPENDIX: ELIMINATION OF PARAMETERS

The starting point is the potential V [Eq. (9)],

$$V=\sum_s\left[\frac{\langle(\mathbf{q}s^\dagger-f_s[\{\mathbf{q}\mathbf{u}^\dagger\}])^2\rangle}{c_s}+\lambda_s[\langle(\mathbf{q}\mathbf{s}^\dagger)^2\rangle-c_s]\right]+\sum_u\frac{\langle(\dot{\mathbf{q}}\mathbf{u}^\dagger-f_u[\{\mathbf{q}\mathbf{u}^\dagger\}])^2\rangle}{\langle(\dot{\mathbf{q}}\mathbf{u}^\dagger)^2\rangle}\,, \tag{A1}$$

with λ_s representing a Lagrange parameter fixing scaling of $\mathbf{s}^\dagger$ and f_s and f_u being nonlinear functions in $\mathbf{u}^\dagger$

$$f_s[\{\mathbf{q}\mathbf{u}^\dagger\}]=\sum_{u,u'}k^{(2)}_{suu'}\mathbf{q}\mathbf{u}^\dagger\mathbf{q}\mathbf{u}'^\dagger+\sum_{u,u',u''}k^{(3)}_{suu'u''}\mathbf{q}\mathbf{u}^\dagger\mathbf{q}\mathbf{u}'^\dagger\mathbf{q}\mathbf{u}''^\dagger+\cdots\,,$$

$$f_u[\{\mathbf{q}\mathbf{u}^\dagger\}]=a^{(0)}_u+a^{(1)}_u\mathbf{q}\mathbf{u}^\dagger+\sum_{u',u''}a^{(2)}_{uu'u''}\mathbf{q}\mathbf{u}'^\dagger\mathbf{q}\mathbf{u}''^\dagger+\sum_{u',u'',u'''}a^{(3)}_{uu'u''u'''}\mathbf{q}\mathbf{u}'^\dagger\times\mathbf{q}\mathbf{u}''^\dagger\mathbf{q}\mathbf{u}'''^\dagger+\cdots\,.$$

(a) Variation of the potential [Eq. (A1)] with respect to $\mathbf{s}^\dagger, k^{(2)}_{su_1u_2}, k^{(3)}_{su_1u_2u_3}$ yields,

$$\langle((1+c_s\lambda_s)\mathbf{q}\mathbf{s}^\dagger-f_s[\{\mathbf{q}\mathbf{u}^\dagger\}])\mathbf{q}\rangle=0\,,$$

$$\langle((\mathbf{q}\mathbf{s}^\dagger)-f_s[\{\mathbf{q}\mathbf{u}^\dagger\}])(\mathbf{q}\mathbf{u}_1^\dagger)(\mathbf{q}\mathbf{u}_2^\dagger)\rangle=0\,,$$

$$\langle((\mathbf{q}\mathbf{s}^\dagger)-f_s[\{\mathbf{q}\mathbf{u}^\dagger\}])(\mathbf{q}\mathbf{u}_1^\dagger)(\mathbf{q}\mathbf{u}_2^\dagger)(\mathbf{q}\mathbf{u}_3^\dagger)\rangle=0\,,$$

which represents a homogeneous linear set of equations for the variables $\mathbf{x}$,

$$\mathbf{x}=(\mathbf{s}^\dagger,k^{(2)}_{suu'},k^{(3)}_{suu'u''})^T\,,$$

as a function of $\{\mathbf{u}^\dagger\}$

$$L[\lambda_s,\{\mathbf{u}^\dagger\}]\mathbf{x}=\mathbf{0}\,, \tag{A2}$$

with

$$L[\lambda_s,\{\mathbf{u}^\dagger\}]=\begin{pmatrix}(1+c_s\lambda_s)\Gamma_2 & -\Gamma_3{:}\mathbf{u}^\dagger{:}\mathbf{u}'^\dagger & -\Gamma_4{:}\mathbf{u}^\dagger{:}\mathbf{u}'^\dagger{:}\mathbf{u}''^\dagger\\ -\Gamma_3{:}\mathbf{u}_1^\dagger{:}\mathbf{u}_2^\dagger & -\Gamma_4{:}\mathbf{u}^\dagger{:}\mathbf{u}'^\dagger{:}\mathbf{u}_1^\dagger{:}\mathbf{u}_2^\dagger & -\Gamma_5{:}\mathbf{u}^\dagger{:}\mathbf{u}'^\dagger{:}\mathbf{u}''^\dagger{:}\mathbf{u}_1^\dagger{:}\mathbf{u}_2^\dagger\\ -\Gamma_4{:}\mathbf{u}_1^\dagger{:}\mathbf{u}_2^\dagger{:}\mathbf{u}_3^\dagger & -\Gamma_5{:}\mathbf{u}^\dagger{:}\mathbf{u}'^\dagger{:}\mathbf{u}_1^\dagger{:}\mathbf{u}_2^\dagger{:}\mathbf{u}_3^\dagger & -\Gamma_6{:}\mathbf{u}^\dagger{:}\mathbf{u}'^\dagger{:}\mathbf{u}''^\dagger{:}\mathbf{u}_1^\dagger{:}\mathbf{u}_2^\dagger{:}\mathbf{u}_3^\dagger\end{pmatrix}$$

We used the notation of higher order correlation tensors introduced in Sec. IV. To obtain nontrivial solutions, the determinant of the matrix $L[\lambda_s,\{\mathbf{u}^\dagger\}]$ has to vanish, which leads to an equation for the Lagrange parameters λ_s

$$\det L[\lambda_s,\{\mathbf{u}^\dagger\}]=0 \Longrightarrow \lambda_s=\lambda_s[\{\mathbf{u}^\dagger\}] . \tag{A3}$$

Inserting Eq. (A3) back into the homogeneous set of Eqs. (A2), and solving for $\mathbf{x}$, one obtains the variables, $s^\dagger, k^{(2)}_{su_1u_2}, k^{(3)}_{su_1u_2u_3}$, as a function of $\{\mathbf{u}^\dagger\}$

$$\mathbf{x}=\mathbf{x}[\{\mathbf{u}^\dagger\}] . \tag{A4}$$

(b) Variation of the potential [Eq. (A1)] with respect to $a^{(0)}_u$, $a^{(1)}_u$, $a^{(2)}_{uu_1u_2}$, $a^{(3)}_{uu_1u_2u_3}$ yields,

$$\langle(\dot{\mathbf{q}}\mathbf{u}^\dagger - f_u[\{\mathbf{q}\mathbf{u}^\dagger\}])\rangle=0 ,$$
$$\langle(\dot{\mathbf{q}}\mathbf{u}^\dagger - f_u[\{\mathbf{q}\mathbf{u}^\dagger\}])\mathbf{q}\mathbf{u}^\dagger\rangle=0 ,$$
$$\langle(\dot{\mathbf{q}}\mathbf{u}^\dagger - f_u[\{\mathbf{q}\mathbf{u}^\dagger\}])(\mathbf{q}\mathbf{u}_1^\dagger)(\mathbf{q}\mathbf{u}_2^\dagger)\rangle=0 ,$$
$$\langle(\dot{\mathbf{q}}\mathbf{u}^\dagger - f_u[\{\mathbf{q}\mathbf{u}^\dagger\}])(\mathbf{q}\mathbf{u}_1^\dagger)(\mathbf{q}\mathbf{u}_2^\dagger)(\mathbf{q}\mathbf{u}_3^\dagger)\rangle=0 ,$$

which represents a nonhomogeneous linear set of equations for the variables $\mathbf{a}$,

$$\mathbf{a}=(a^{(0)}_u, a^{(1)}_u, a^{(2)}_{uu_1u_2}, a^{(3)}_{uu_1u_2u_3})^T ,$$

as a function of $\{\mathbf{u}^\dagger\}$:

$$M[\{\mathbf{u}^\dagger\}]\mathbf{a}=\mathbf{y}[\{\mathbf{u}^\dagger\}] , \tag{A5}$$

with

$$M[\{\mathbf{u}^\dagger\}]=\begin{pmatrix} 1 & \Gamma_1:\mathbf{u}^\dagger & \Gamma_2:\mathbf{u}'^\dagger:\mathbf{u}''^\dagger & \Gamma_3:\mathbf{u}'^\dagger:\mathbf{u}''^\dagger:\mathbf{u}'''^\dagger \\ \Gamma_1:\mathbf{u}^\dagger & \Gamma_2(:\mathbf{u}^\dagger)^2 & \Gamma_3:\mathbf{u}^\dagger:\mathbf{u}'^\dagger:\mathbf{u}''^\dagger & \Gamma_4:\mathbf{u}^\dagger:\mathbf{u}'^\dagger:\mathbf{u}''^\dagger:\mathbf{u}'''^\dagger \\ \Gamma_2:\mathbf{u}_1^\dagger:\mathbf{u}_2^\dagger & \Gamma_3:\mathbf{u}^\dagger:\mathbf{u}_1^\dagger:\mathbf{u}_2^\dagger & \Gamma_4:\mathbf{u}'^\dagger:\mathbf{u}''^\dagger:\mathbf{u}_1^\dagger:\mathbf{u}_2^\dagger & \Gamma_5:\mathbf{u}'^\dagger:\mathbf{u}''^\dagger:\mathbf{u}'''^\dagger:\mathbf{u}_1^\dagger:\mathbf{u}_2^\dagger \\ \Gamma_3\cdots & \Gamma_4\cdots & \Gamma_5\cdots & \Gamma_6\cdots \end{pmatrix}$$

and

$$y[\{\mathbf{u}^\dagger\}]=(\Lambda_1:\mathbf{u}^\dagger, \Lambda_2(:\mathbf{u}^\dagger)^2, \Lambda_3:\mathbf{u}^\dagger:\mathbf{u}_1^\dagger:\mathbf{u}_2^\dagger, \Lambda_4:\mathbf{u}^\dagger:\mathbf{u}_1^\dagger:\mathbf{u}_2^\dagger:\mathbf{u}_3^\dagger)^T .$$

For sets of vectors $\{\mathbf{u}^\dagger\}$ with $\det M[\{\mathbf{u}^\dagger\}]\neq 0$, Eq. (A5) can be inverted, and we obtain the variables, $a^{(0)}_u$, $a^{(1)}_u$, $a^{(2)}_{uu_1u_2}$, $a^{(3)}_{uu_1u_2u_3}$, as a function of $\{\mathbf{u}^\dagger\}$:

$$\mathbf{a}=\mathbf{a}[\{\mathbf{u}^\dagger\}]=M^{-1}[\{u^\dagger\}]\mathbf{y}[\{\mathbf{u}^\dagger\}] . \tag{A6}$$

Inserting finally Eqs. (A4) and (A6) into Eq. (A1), we end up with a potential V depending on $\{\mathbf{u}^\dagger\}$ only,

$$V=V[\{\mathbf{u}^\dagger\}] ,$$

which corresponds to Eq. (11) of Sec. III C.

[1] G. Berkooz, P. Holmes, and J. L. Lumley, Annu. Rev. Fluid Mech. **25**, 539 (1993).
[2] G. Plaut and R. Vautard, J. Atmos. Sci. **51**, 210 (1994).
[3] R. Friedrich and C. Uhl, in *Evolution of Dynamical Structures in Complex Systems,* edited by R. Friedrich and A. Wunderlin (Springer-Verlag, Berlin, 1992).
[4] D. Gallez and A. Babloyantz, Biol. Cybern. **64**, 381 (1991).
[5] A. Fuchs, J. A. S. Kelso, and H. Haken, Int. J. Bifurcation Chaos **2**, 917 (1992).
[6] V. K. Jirsa, R. Friedrich, H. Haken, and J. A. S. Kelso, Biol. Cybern. **71**, 27 (1994).
[7] H. Haken, *Information and Selforganization* (Springer-Verlag, Berlin, 1988).
[8] P. Grassberger and I. Procaccia, Physica D **9**, 189 (1983).
[9] F. Takens, in *Dynamical Systems and Turbulence,* edited by D. Rand and L. S. Young (Springer, Berlin, 1981).
[10] D. S. Broomhead and G. P. King, Physica D **20**, 217 (1987).
[11] H. D. I. Abarbanel, R. Brown, J. J. Sidorowich, and L. S. Tsimring, Rev. Mod. Phys. **65**, 1331 (1993).
[12] E. Baake, M. Baake, H. G. Bock, and K. M. Briggs, Phys. Rev. A **45**, 5524 (1992).
[13] S. P. Layne, G. Mayer-Kress, and J. Holzfuss, in *Dimensions and Entropies in Chaotic Systems,* edited by G. Mayer-Kress (Springer-Verlag, Berlin, 1986).
[14] M. Paluš and I. Dvořák, Physica D **55**, 221 (1992).
[15] J. P. Eckmann and D. Ruelle, Physica D **56**, 185 (1992).
[16] A. Armbruster, R. Heiland, and E. J. Kostelich, Chaos **4(2)**, 421 (1994).
[17] C. Uhl, R. Friedrich, and H. Haken, Z. Phys. B **92**, 211 (1993).
[18] H. Haken, *Synergetics. An Introduction,* 3rd ed. (Springer-Verlag, Berlin, 1983).
[19] H. Haken, *Advanced Synergetics,* 3rd ed. (Springer-Verlag, Berlin, 1993).
[20] J. Fineberg, E. Moses, and V. Steinberg, Phys. Rev. Lett. **61**, 838 (1988); P. Kolodner and C. M. Surko, *ibid.* **61**, 842 (1988).
[21] M. Bestehorn, R. Friedrich, and H. Haken, Z. Phys. B **77**, 151 (1989); M. Bestehorn, R. Friedrich, and H. Haken, Physica D **37**, 295 (1989).
[22] M. Kirby, Physica D **57**, 466 (1992).

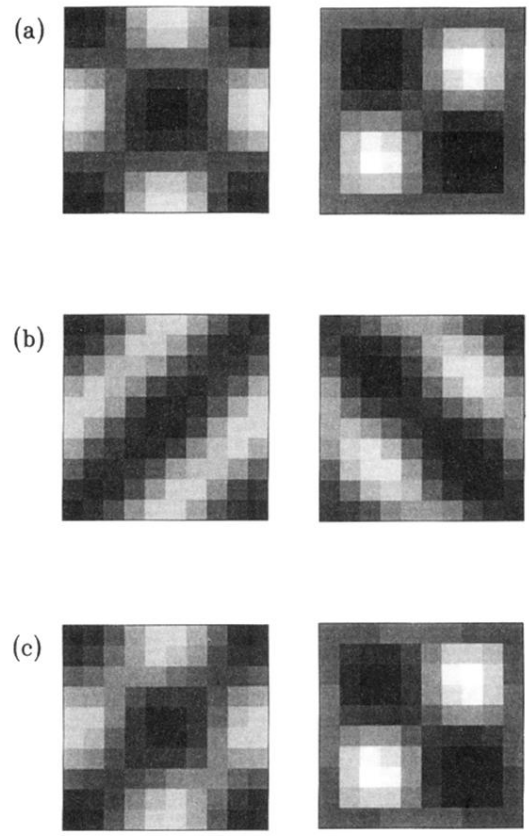

FIG. 2. (a) Simulated spatial modes $\tilde{\mathbf{u}}$ and $\tilde{\mathbf{s}}$, (b) the resulting two vectors of PCA, and (c) modes, obtained by our method.

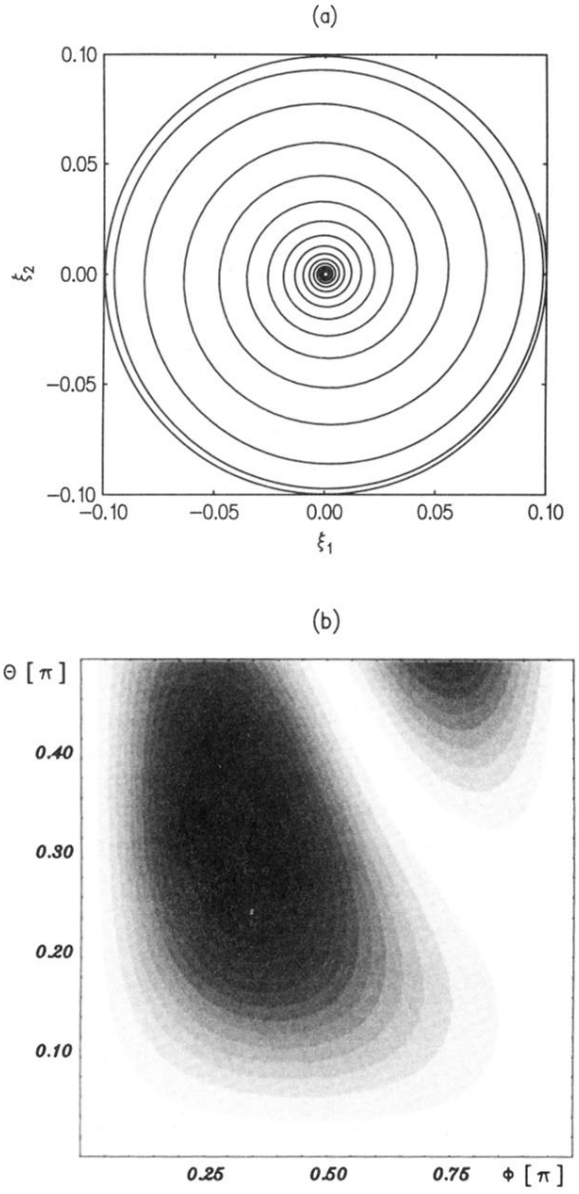

FIG. 4. (a) Phase portrait of the amplitudes $\xi_1(t)$ and $\xi_2(t)$ of a simulated super-critical Hopf bifurcation [Eq. (32), $\epsilon=0.05$, $\omega=1$, $a=-5$, and $b=75$]. (b) Two-dimensional least-square-fit potential $V_u(\phi,\theta)$ corresponding to the simulated Hopf bifurcation. The values of the potential $V(\phi,\theta)$ are given by different grey values: Black represents the minimum of the potential, white the maximum. The potential shows one distinct minimum and the expected symmetry $V(\phi-\pi/2,\theta=\pi/2)$ $=V(\phi+\pi/2,\theta=\pi/2)$.

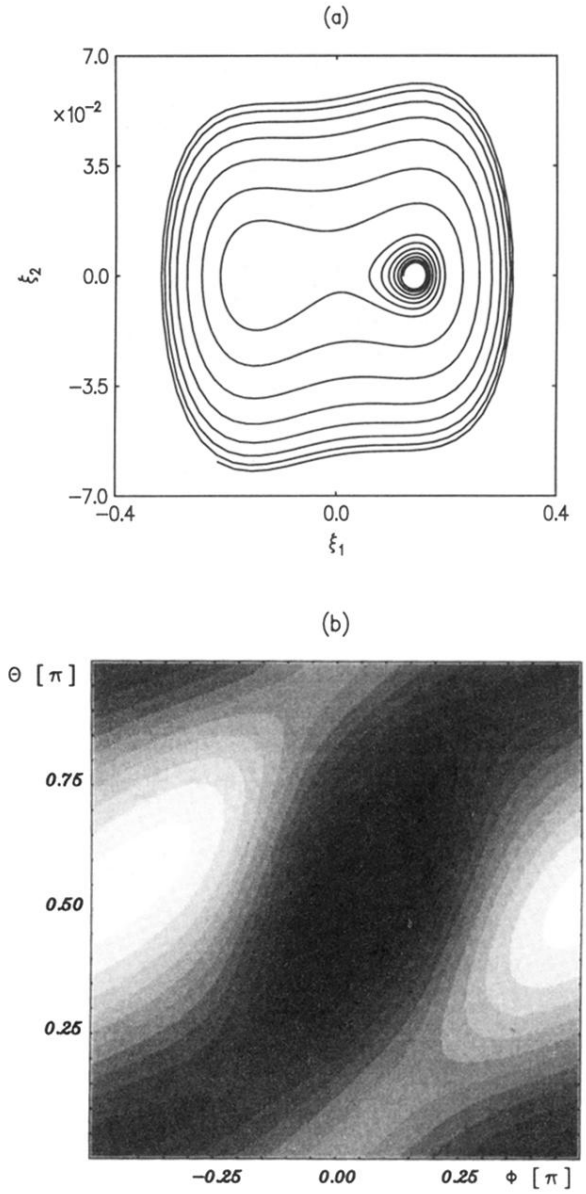

FIG. 5. (a) Phase portrait of the amplitudes $\xi_1(t)$ and $\xi_2(t)$ of a simulated codimension-two bifurcation [Eq. (46), $\mu_1=0.02$, $\mu_2=0.03$, $c=-1$]. (b) Least-square-fit potential $V_u(\phi,\theta)$ corresponding to the simulated codimension-two bifurcation with the same color coding as in Fig. 4(b). There occurs again one distinct minimum and the expected symmetry of a torus.